AIAA JOURNAL
Vol. 36, No. 2, February 1998

Sensor Placement Methodologies for Dynamic Testing

Michael Papadopoulos* and Ephrahim Garcia†
Vanderbilt University, Nashville, Tennessee 37235

Two methods are presented for structural sensor placement. The first scheme selects the most linearly independent impulse responses at all candidate sensor locations from a Gram–Schmidt orthogonalization procedure. The second scheme is based on a principal component analysis and iteratively removes sensors that do not contribute significant information to the Fisher information matrix. Furthermore, use of a model reduction criterion is proposed to address the optimality issue. Several sensor placement methods were implemented to compare results and were applied to an Euler–Bernoulli beam and a cantilevered frame structure. It is shown that the proposed frequency criterion appears to be a selective criterion for choosing optimum sensor locations. Finally, the optimum measurement locations from several of the methods studied yield acceptable results based on data from an experimental study on the frame structure.

Introduction

IT is often required to select a predefined number of sensor locations for system identification. These locations should be such that they can recover the target frequencies of interest and faithfully represent the structural mode shapes. In addition, such an analysis proves useful when, for example, performing health monitoring or control. It is desirable to be able to fully instrument a structure. This is so because there will be enough sensors to spatially separate individual modes. However, high costs of data acquisition systems, i.e., accelerometers and supporting instrumentation, etc., and accessibility limitations often constrain the number of sensors. Furthermore, although grounded structures are often simpler to test, it is becoming increasingly important to test structures under operating conditions. Orbiting structures, for example, are not easily amenable to removal and placement of sensors. Finally, even if sufficient instrumentation were possible, it is likely that sensor redundancy would exist. Although this offers advantages, it is of interest to seek as small as possible number of sensors that contain as much information as possible about the target modes.

The sensor placement problem can be approached from several points of view. Several authors have considered an optimum selection from control principles.[1–4] Others have taken a structural dynamic viewpoint from which recovery of modal parameters are of interest.[5–8] Still other approaches can be found in Refs. 9 and 10. A relatively new approach was proposed by Avitabile et al.[11] First, a small modal survey of the structure is conducted. Then, a singular value decomposition is performed on the measured frequency response functions (FRFs) to determine the required number of reference measurements. This is a good approach for two reasons. First, there is no need for an analytical model, which is likely to be in error. Second, actual measurement data are used to determine the optimum measurement locations. A drawback is that it does require a preliminary modal test, which, for example, is not necessarily feasible for orbiting structures. Methods based exclusively on analytical models will now be discussed.

The simplest sensor placement method is to visually inspect the mode shapes of interest and select points with high amplitude. This is the visual inspection (VI) method, and although efficient, it is practical only for simple structures. More quantitative methods along these lines can be found in Refs. 12 and 13, which introduce the concept of modal windows. Another effective visual inspection technique is the modal kinetic energy (MKE).[14–16] An MKE plot for each target mode is generated for every candidate sensor location. The location with the largest energy over all target modes is selected. The principle behind this is that locations with high MKE serve as good sensors due to the large motion. One drawback of the MKE method is that it is highly dependent on the finite element mesh size. That is, it picks locations in coarser mesh regions where the mass is larger. A similar computation to the MKE is the driving point residue (DPR).[15,16] The DPR is a measure of a particular degree of freedom (DOF) location at exciting a particular mode. The points with a large DPR value are selected.

Automated procedures, however, are more attractive inasmuch as there is less user input. The average modal kinetic energy (AMKE) method[15,16] simply computes the average kinetic energy (AKE) over all target modes. The desired number of sensors is then selected from the larger AKE values. One advantage of this method is that it smears the effect of nodal points that have zero motion. An alternative to avoid selecting nodal points is the eigenvector component product (ECP).[15] This method computes the product of the finite element (FE) target mode shapes at the candidate sensor DOFs. All locations that have large product values are taken as the optimum sensors. An average driving point residue (ADPR)[16] can also be calculated. And like AMKE, it is an average of the DPR across the rows. The larger ADPR values serve as the sensor locations. Chung and Moore[16] also use weighted versions of AMKE (WAMKE) and ADPR (WADPR) to discriminate against DOFs with zero motion.

These schemes all rely on an analytical model. Pape's[17] Chebyshev interpolation (CI) technique, like that in Ref. 11, avoids this requirement. It chooses the locations as the roots of Chebyshev polynomials. The basis for this is that the maximum error in interpolating a set of target mode shapes is minimal when the sample points are the zeros of the Chebyshev polynomials. The only difficulty with CI is that it is generally applicable to simple one- or two-dimensional structures. The VI, MKE, AMKE, WAMKE, ECP, DPR, ADPR, WADPR, and CI methods are noniterative techniques. That is, an optimum sensor set is found immediately after computing the appropriate values.

Several recently developed iterative techniques will now be discussed. Kammer's effective independence (EFI) method[14] ranks sensor locations to their independence of the target modal matrix. The idea is to eliminate DOFs that do not contribute to the independence of the target mode shapes. An alternative formulation is that due to Tasker and Liu.[18] They suggest a variance-based EFI (VEFI) method, where DOFs are eliminated that have a small variance in the parameter estimates. Another related scheme is to mass weight the modal matrix before computing the effective independence value.[19] Several weaknesses of EFI, as noted by Poston,[20] are as follows: 1) it does not take into account the geometry of the structure and, thus, yields sensor locations that contribute redundant information, 2) there is no consideration of time information, 3) there is no indication

Received May 17, 1996; revision received Aug. 5, 1997; accepted for publication Sept. 22, 1997.

*Graduate Research Assistant, Department of Mechanical Engineering, Smart Structures Laboratory; currently Member of Technical Staff, Structural Technology Department, The Aerospace Corporation, El Segundo, CA 90245.

†Associate Professor, Department of Mechanical Engineering, Smart Structures Laboratory, Box 1592, Station B. Member AIAA.

as to the number of sensors that can be removed at each iteration, and 4) there is no indication as to the final number of sensors that should be retained in the final sensor set.

Park and Kim,[21] however, not only derive a method that makes the target modal matrix as independent as possible but also present a guide for the allowable number of deleted DOFs at each iteration. The method relies on computing a singular value decomposition (SVD) of the target modal matrix and evaluates the Fisher information matrix (FIM). Then, DOFs are eliminated that have no effect on the determinant of the FIM. Penny et al.[22,23] take a model reduction viewpoint, which is related to that presented by Henshell and Ong[24] and Shah and Raymund.[25] A ratio of the diagonal elements of the stiffness matrix to the diagonal elements of the mass matrix is computed. The DOF with the largest ratio value is then eliminated. The system is then Guyan[26] reduced, and the process repeated. The Guyan reduction (GR) approach maintains accuracy of the lower system modes, which do not necessarily have to represent the set of target modes. In this regard, this is a limitation on the method. An alternate approach in performing GR at each iteration is the use of less approximate reduction methods, such as the improved reduced system (IRS)[27] or successive approximate reduction (SAR).[28]

In keeping with retaining DOFs that contain as much modal information as possible, Flanigan and Botos[29] suggest using static flexibility shapes evaluated at the candidate DOF. The optimal DOFs are then iteratively identified for which a linear combination of flexibility shapes matches as closely as possible to the set of target mode shapes. This approach is here designated as the static flexibility (SF) method and was applied to the space station combined cargo element in Ref. 30. Lim,[31] however, selects sensors that minimize the condition number of the Hankel matrix of impulse responses. This method will be called the modal parameter identification (MPI) method because the Hankel matrix is used in modal parameter identification algorithms, such as the eigensystem realization algorithm (ERA).[32]

One method is proposed in this paper to address the sensor redundancy issue in the EFI method. It computes the impulse response at all candidate DOFs, and then ranks the sensor locations according to the independence of the measurements. That is, a matrix of impulse responses is formed and the Gram–Schmidt (G–S) orthogonalization procedure is used to rank the sensors based on the measurement magnitude after each orthogonalization. In this manner, only the sensors locations that produce the most independent measurements are used. Unlike the previous methods, which make the target modal matrix as independent as possible, this G–S method makes the measurement matrix as independent as possible. Consequently, the larger measurement magnitude DOFs will produce a well-conditioned Hankel matrix in ERA. A variant of this approach is to compute the least correlated sensor DOF at each iteration instead of performing an orthogonalization. An alternate method is based on a principal component analysis.[33] In this method, an eigenanalysis on the transpose of the FIM is computed. The smallest component DOF (in absolute value) from the eigenvector associated with the smallest eigenvalue is eliminated. The process is repeated until the desired number of sensors remain. The advantage of this method is that the DOF with the largest information in the FIM is retained in the next iteration.

The different sensor placement methods have just been discussed. But there still lacks a criterion to judge the quality of the chosen measurement locations. This ultimately leads to the issue on whether there truly exists an optimal sensor set. That is, with the multitude of sensor placement schemes comes a multitude of sensor locations, which all claim optimality or suboptimality in one way or another. Although all of the discussed methods typically yield acceptable locations, they do not necessarily yield the optimum set. Penny et al.[23] discuss and assess five criteria, the modal assurance criterion, the modified modal assurance criterion, the SVD ratio, the measured energy per mode, and the determinant of the FIM, and attempt to address the quality of the chosen measurement locations. They suggest the SVD ratio as the best criterion among the examples considered.[23] This paper proposes that the optimum sensor set is one that maximizes the lowest eigenvalue of the system comprising the deleted DOFs. This is the criterion[24] that must be satisfied if the reduced mass and stiffness matrices are to faithfully maintain the accuracy of the lower system modes in a model reduction. This is expected to be a quality criterion provided the lower modes are indeed the target modes.

Each of the sensor placement methods were implemented on an Euler–Bernoulli beam model, a plate model of a wing structure, and a cantilevered frame structure. Furthermore, experimental data available on the frame structure are used to validate the selected sensor locations for several of the methods. Each of the sensor placement methods is now briefly discussed, along with the SVD ratio and the proposed model reduction criterion for quantifying the optimum sensor set.

Problem Formulation

Sensor Placement Methods

MKE[14–16]

Given a target modal matrix Φ_{tm} of size $n \times m$, where n is the total number of FE DOFs and m is the number of target modes, the MKE is given as

$$\text{MKE} = \Phi_{tm} \otimes M\Phi_{tm} \tag{1}$$

where $\otimes$ denotes element by element multiplication. The candidate DOFs with consistently large kinetic energy values over all of the target modes (columns in MKE) are taken to be the optimum sensor set. The idea here is the DOF with the largest kinetic energy will ultimately have the greatest response from which the best possible chance at modal parameter identification is produced.

AMKE

The AMKE[14–16] is simply the average taken across the rows of MKE in Eq. (1), i.e.,

$$\mathbf{AMKE}_i = \frac{1}{m}\sum_{j=1}^{m} \text{MKE}_{ij}, \qquad i = 1, \ldots, n \tag{2}$$

where i is ith candidate DOF. The optimum sensors are the ones with the largest **AMKE** values over the candidate DOF. This approach is more automatic and takes into account any zero motion DOF.

WAMKE

The WAMKE[16] value is computed from the following:

$$\text{WAMKE} = \text{MKE}_{\min} \otimes \mathbf{AMKE} \tag{3}$$

where $\text{MKE}_{\min}$ is the minimum in absolute value across the rows in MKE in Eq. (1). The optimum sensors are the ones with the largest **WAMKE** values over the candidate DOF.

DPR

The DPR[16] is computed from

$$\text{DPR} = \Phi_{tm} \otimes \Phi_{tm}\Omega_{tm} \tag{4}$$

where Ω_{tm} is the $m \times m$ diagonal matrix of target frequencies. The optimum sensors are the ones with consistently large DPR values across the rows for the candidate DOF.

ADPR

The ADPR[16] is similarly computed as in AMKE from

$$\text{ADPR}_i = \frac{1}{m}\sum_{j=1}^{m} \text{DPR}_{ij}, \qquad i = 1, \ldots, n \tag{5}$$

The optimum sensors are the ones with the largest ADPR values over the candidate DOF.

WADPR

The WADPR[16] value is computed from the following:

$$\mathbf{WADPR} = \text{DPR}_{\min} \otimes \text{ADPR} \tag{6}$$

where $\text{DPR}_{\min}$ is the minimum in absolute value across the rows in DPR in Eq. (4). The optimum sensors are the ones with the largest **WAMKE** values over the candidate DOF.

ECP

ECP[15] is the product over all of the target modes. The candidate DOFs with the largest ECP values are selected. The concept here is

Table 1 Roots of the Chebyshev polynomials

	m					
n	0	1	2	3	4	5
0	0					
1	0.71	−0.71				
2	0.87	0	−0.87			
3	0.92	0.38	−0.38	−0.92		
4	0.95	0.59	0	−0.59	−0.95	
5	0.97	0.71	0.26	−0.26	−0.71	−0.97

again to avoid selecting zero motion DOF, which will hamper the modal identification process.

CI

The roots of the Chebyshev polynomial[17] of degree j serve as the sensor locations and are obtained from

$$\varsigma_i = \cos\left[\left(\frac{2i+1}{2j+2}\right)\pi\right], \qquad i = 0, 1, \ldots, j \tag{8}$$

Table 1 lists the roots from the first six Chebyshev polynomials. Because the roots vary from −1 to 1, the mapping onto a one-dimensional region, $a \le x \le b$, is given as

$$x_i = \tfrac{1}{2}[(b-a)\varsigma_i + b + a] \tag{9}$$

The two-dimensional mapping for the region $a \le x \le b$ and $c \le y \le d$ is given in Eq. (9) for x and Eq. (9) for y with a substitution of a for c and b for d. One simply selects the roots down the list in Table 1 until the desired number of sensors Ns is reached.

EFI Without Mass Weighting

The EFI method[14] eliminates sensors with the smallest contribution to the linear independence of the effective independence matrix E. The approach is to eliminate DOFs that do not deteriorate the determinant of the FIM. Matrix E is computed from

$$E = \Phi^r_{\text{tm}} A^{-1} \left(\Phi^r_{\text{tm}}\right)^T \tag{10}$$

where A is the FIM and is evaluated as

$$A = \left(\Phi^r_{\text{tm}}\right)^T \Phi^r_{\text{tm}} \tag{11}$$

and Φ^r_{tm} denotes the target modal matrix reduced to the candidate sensor DOFs. That is, only the candidate DOFs are kept from Φ_{tm}. The procedure is as follows. After computing matrix E, the DOF with the smallest diagonal term of E is eliminated. The appropriate row in Φ^r_{tm} is then removed, Eqs. (10) and (11) are recomputed, and a new DOF is chosen for elimination. The process repeats until the Ns desired DOFs remain. The EFI method without mass weighting is designated EFI W/OM.

EFI with Mass Weighting

Instead of simply removing rows from Φ^r_{tm}, Garvey et al.[19] implement a Guyan reduced mass weighted version of Kammer's EFI method; hence, it is designated EFI W/M. The mass weighted matrix E becomes

$$E = M_G^{0.5} \Phi^r_{\text{tm}} A^{-1} \left(\Phi^r_{\text{tm}}\right)^T M_G^{0.5} \tag{12}$$

where A is computed as

$$A = \left(\Phi^r_{\text{tm}}\right)^T M_G \Phi^r_{\text{tm}} \tag{13}$$

and M_G denotes the Guyan reduced mass matrix at each iteration. First, the full FE mass and stiffness matrices are Guyan reduced to the candidate DOF. Then, Eqs. (12) and (13) are computed, and the DOF with the smallest diagonal term of E is eliminated. That is, the row corresponding to the eliminated DOF is Guyan reduced from the previously reduced mass and stiffness matrices. The process then selects another DOF for elimination. This is repeated until the desired Ns DOFs remain.

VEFI

Tasker and Liu[18] derive an alternate EFI method in which sensors with the smallest variance are eliminated from Φ^r_{tm}. The procedure begins by computing the variance equation,

$$\boldsymbol{\Delta}_i \sigma^2 = \frac{\left[\Phi^r_{\text{tm}} \left(\Phi^r_{\text{tm}}\right)^T\right]^+_{ii}}{\left[I - \Phi^r_{\text{tm}} \left(\Phi^r_{\text{tm}}\right)^+\right]_{ii}} \tag{14}$$

where $(\cdot)^+$ is the pseudoinverse of $(\cdot)$, $[\cdot]_{ii}$ is the iith element of $[\cdot]$, $[\cdot]^+_{ii}$ is the iith element of the pseudoinverse of $[\cdot]$, and I is an appropriately sized identity matrix. The DOF with the smallest $\boldsymbol{\Delta}_i \sigma^2$ is selected for elimination, from which the appropriate row in Φ^r_{tm} is removed, and Eq. (14) is again evaluated. The process repeats until the desired Ns DOFs remain.

SVD

In an analysis similar to the EFI method, Park and Kim[21] also maximize the determinant of the FIM with respect to the retained DOF. However, they use an SVD to identify DOFs that offer little contribution to the determinant. First, the target modal matrix is reduced to the candidate DOF yielding Φ^r_{tm}. Then, the SVD is applied, resulting in

$$\Phi^r_{\text{tm}} = PDQ^T \tag{15}$$

The following residual matrix R is computed:

$$R = \text{diag}(PP^T) \tag{16}$$

and the row with the smallest R value is selected for elimination. The appropriate row in Φ^r_{tm} is then removed, the SVD is recomputed from Eq. (15), and matrix R is formed in Eq. (16) from which a new DOF is eliminated. The process repeats until the desired Ns DOFs remain.

GR

The preceding iterative methods all preserve the determinant of FIM in an attempt to keep as much information as possible in the remaining DOFs. Penny et al.,[22,23] however, adopt a model reduction viewpoint. That is, they assume that the master DOFs associated with a model reduction can serve as good sensor locations. This approach is effective only if the lower modes of the system are considered in the target modal matrix. To preserve the lower system modes in a model reduction, DOFs should be eliminated with a high stiffness and low inertia. Then the ratio of the diagonal elements of the stiffness and mass matrices quantifies the importance of each DOF. A lower ratio indicates a DOF with significant inertia effects. Alternatively, a larger ratio indicates a DOF with significant stiffness effects. The procedure is as follows. First, the full FE mass and stiffness is Guyan reduced to the candidate DOF. The stiffness-mass ratio is then computed as

$$\boldsymbol{R}_i = K_{G_{ii}} / M_{G_{ii}} \tag{17}$$

where K_G and M_G are Guyan reduced stiffness and mass matrices, respectively. The DOF with the largest $\boldsymbol{R}_i$ value is selected for elimination. The corresponding row in the previously obtained reduced matrices is then Guyan reduced out and a new $\boldsymbol{R}_i$ ratio is computed, from which another DOF is selected. The process repeats until the desired Ns DOFs remain.

IRS

The GR sensor placement method assumes that the master DOF can represent a good sensor set. The slave DOFs were selected such that the ratio of stiffness to mass is large. This ratio was determined after a static reduction in each iteration. Because the GR can be very approximate, the final master DOF set can be in error. Using a more exact model reduction scheme may be advantageous because the dynamic behavior from each iteration is more likely to be preserved. The IRS method[27] is one such formulation. Therefore, the procedure for this method is the same as the GR approach except that the IRS technique is substituted for Guyan.

SAR

The SAR[28] is yet another more exact reduction technique that can be substituted for Guyan in the GR method. In terms of preserving

the original dynamic behavior, the SAR method does better than IRS, which does better than Guyan.

SF

The SF approach[29] also takes a model reduction viewpoint. That is, it is based on the premise that the best master DOFs for a test-analysis model are the ones that contain as much information as possible on the target mode shapes. The underlying assumption is that the best master DOFs are such that a linear combination of static flexibility shapes obtained from a stiffness matrix reduced to those DOFs matches the FE target mode shapes. The method begins by applying unit loads at all candidate DOFs and solving

$$\begin{bmatrix} K_{mm} & K_{ms} \\ K_{sm} & K_{ss} \end{bmatrix} \Psi = \begin{bmatrix} I_m \\ 0 \end{bmatrix} \tag{18}$$

where K is partitioned into its master (m) and slave (s) DOFs and I_m is the $m \times m$ identity matrix. The static flexibility matrix Ψ is then written as a linear combination of the target modal matrix

$$\Psi Q = \Phi_{tm} \tag{19}$$

The matrix Q is then solved (using a pseudoinverse, for example) and normalized such that the sum of the absolute values for each column is unity. Then a DOF weighting is calculated by summing the absolute values across all of the rows. The DOF with the smallest weight is eliminated. Therefore, the stiffness matrix in Eq. (18) is repartitioned with the new master DOF and a new matrix Q is computed, from which the DOF with the smallest weight is again removed. The process is repeated until the desired Ns DOFs is reached.

MPI

The optimum sensors are selected such that it minimizes the condition number of a Hankel matrix of pulse responses. Because the Hankel matrix is used for modal extraction from time-domain system identification methods, it is expected that a well-conditioned (and full rank) Hankel matrix will recover the target modes. Furthermore, instead of computing an effective independence of the FIM as in EFI, MPI[31] uses an effective independence of the Hankel matrix itself. Therefore, sensors that contribute little to no information in the Hankel matrix are eliminated. The method begins by constructing a state-space model of the target modes. First, the target modal matrix is mass normalized such that $\Phi_{tm}^T M \Phi_{tm} = I$. The continuous state-space model then becomes

$$A_c = \begin{bmatrix} 0 & I \\ -\Omega_{tm}^2 & -2Z\Omega_{tm} \end{bmatrix}, \qquad B_c = \begin{bmatrix} 0 \\ \Phi_{tm}^T B_f \end{bmatrix}$$
$$C = \Phi_{tm}^r \begin{bmatrix} -\Omega_{tm}^2 & -2Z\Omega_{tm} \end{bmatrix} \tag{20}$$

where Z is an $m \times m$ diagonal matrix of specified modal damping ratios (typically 1%, if unknown), the $n \times n_a$ matrix B_f identifies the input locations where n_a is the number of inputs, and the NCS $\times m$ Φ_{tm}^r matrix is the mass normalized target modal matrix reduced to the candidate DOF, where NCS is the number of candidate (NCS) DOF. Matrices A_c and B_c are then transformed to discrete time:

$$A = e^{A_c \Delta t}, \qquad B = \left(\int_0^{\Delta t} e^{A_c s}\, ds \right) B_c \tag{21}$$

where Δt is the sampling time. The controllability W and observability V matrices are then computed:

$$W = [B \quad AB \quad \cdots \quad A^{m-n_a} B], \qquad V = \begin{bmatrix} C \\ CA \\ \vdots \\ CA^m \end{bmatrix} \tag{22}$$

from which the Hankel matrix H can be constructed as

$$H = VW \tag{23}$$

Each DOF is then ranked according to its contribution to the rank of H. The contribution of the jth row of H to the total rank is given by

$$\boldsymbol{eh}_j = (HH^+)_{jj} \tag{24}$$

where superscript + denotes the pseudoinverse and $(\cdot)_{jj}$ denotes the jjth element of $(\cdot)$. The effective independence of the ith sensor to H is then

$$\boldsymbol{es}_i = \sum_{k=1}^{m+1} eh_{i+(k-1)\text{NCS}} \tag{25}$$

At each iteration, a new NCS is computed and, because only one DOF is eliminated per iteration, it is decreased by one per iteration. Finally, the DOF with the smallest $\boldsymbol{es}$ value in Eq. (25) is eliminated. Consequently, new C and V matrices are evaluated from Eqs. (20) and (22), respectively, from which a new Hankel matrix and $\boldsymbol{es}$ vector are computed and another DOF selected for elimination. The process repeats until only the desired Ns DOFs remain.

Gram–Schmidt (G–S1 and G–S2)

As mentioned earlier, the EFI method generally exhibits several weaknesses and includes selecting redundant sensor DOFs and no consideration of time information. The G–S orthogonalization is proposed to overcome these dilemmas. The basic principle is to make a Hankel matrix of impulse responses as linearly independent as possible. In so doing, sensor redundancy is quickly minimized and time data are now brought into the problem. Furthermore, it is assumed that a well-conditioned Hankel matrix is expected from using as linearly independent measurements as possible. Because this type of data matrix is used for modal parameter identification (in ERA, for instance), good results are expected. Kammer's EFI[14] approach can more aptly be defined as an effective mode shape independence method, whereas the G–S approach can be called an effective output independence method.

The procedure begins by generating impulse responses at all candidate sensor DOFs for only the m target modes of interest. A modal damping model is assumed as in MPI (typically 1% damping). The mean is then removed from all measurements. The Hankel matrix is then formed as

$$H = \begin{bmatrix} y_1(0) & y_1(\Delta t) & \cdots & y_1(\ell \Delta t) \\ \vdots & \vdots & \vdots & \vdots \\ y_{\text{NCS}}(0) & y_{\text{NCS}}(\Delta t) & \cdots & y_{\text{NCS}}(\ell \Delta t) \end{bmatrix} \tag{26}$$

where ℓ is the data length. The correlation matrix is then computed:

$$\rho = \begin{bmatrix} 1 & \rho_{12} & \cdots & \rho_{1\text{NCS}} \\ & 1 & \cdots & \rho_{2\text{NCS}} \\ \text{sym} & & \ddots & \vdots \\ & & & 1 \end{bmatrix} \tag{27}$$

where ρ_{ij} is the ijth correlation coefficient between the ith and jth measurements in Eq. (26). The minimally correlated sensor [min $(\bar{\rho})$] is next selected as the reference measurement:

$$\bar{\rho}_j = \sum_{i=1}^{\text{NCS}} |\rho_{ij}|, \qquad j = 1, \ldots, \text{NCS} \tag{28}$$

The modified G–S orthogonalization procedure[34] is performed on Eq. (26), and a new Hankel matrix is formed in which the measurements have been made linearly independent with respect to the first minimally correlated sensor. Each remaining sensor measurement is then ranked according to its magnitude. The maximum magnitude measurement serves as the next reference measurement, and the remaining measurements are made linearly independent with respect to it. The magnitudes are then computed, and the maximum measurement magnitude is again used as the next reference measurement. The process is repeated until all of the measurements have been processed, effectively removing the dependency between the measurements, if any. The final set of sensor locations are then the ones with the maximum magnitudes. Whereas the method is used

for impulse responses, forced data could also be used. However, this was found to yield the same set of locations as when using the impulse data. The alternative to using the magnitude after each orthogonalization as a ranking scheme is to simply take the minimally correlated sensor at each iteration. The final optimum set of locations are then the minimally correlated sensors. The former method is designated as G–S1 whereas the latter is referred to as G–S2. Only m sensor locations will be independent when using G–S1 because only m modes are used to compute the impulse responses. If the number of target modes is less than Ns, then G–S2 can be used for the remaining candidate DOFs impulse responses to select the $(Ns - m)$ minimally correlated sensors. This then represents the G–S1 method.

Principal Component Analysis

The basic premise behind principal component analysis (PCA) is to eliminate irrelevant information. That is, it is designed to keep only the most important information in a data sequence. The proposed method is opposite the concept of subspace decomposition.[33] The method is based on the following idea. Given a zero mean $n \times 1$ random vector $\boldsymbol{x}$, the $n \times n$ correlation matrix is defined as

$$R = E\{\boldsymbol{x}\boldsymbol{x}^T\} \tag{29}$$

where $E\{\cdot\}$ denotes the expectation operator. Computing an eigenanalysis on R yields

$$R\boldsymbol{v} = \lambda\boldsymbol{v} \tag{30}$$

Data reconstruction of $\boldsymbol{x}$ from the eigenvectors and eigenvalues in Eq. (30) is possible and given as

$$\boldsymbol{x} = \sum_{i=1}^{n} a_i v_i \tag{31}$$

where a_i is the ith principal component. From a variance analysis, the following is known:

$$\text{var}(\boldsymbol{x}) = \sum_{i=1}^{n} \lambda_i \tag{32}$$

Equation (32) is a key equation. It states that the variance of $\boldsymbol{x}$ is simply a sum of the eigenvalues and depends more on the higher eigenvalues. As a consequence, if the smallest eigenvalue λ_1 is deleted from the sum, then vector $\boldsymbol{x}$ has not changed statistically because the variance remains almost the same. Therefore, the first eigenvector v_1 could be ignored when reconstructing $\boldsymbol{x}$. Furthermore, the smallest component from v_1 will inherently contain minimal information. The following method is then proposed. Remove the mean from every reduced target mode shape in Φ^r_{tm}. Define the target modal correlation matrix as

$$R_{\text{tm}} = \Phi^r_{\text{tm}}\left(\Phi^r_{\text{tm}}\right)^T \tag{33}$$

Compute the eigenvector associated with the smallest eigenvalue and iteratively delete sensor DOFs with the smallest eigenvector component in absolute value. Then recompute the smallest eigenvector and select the DOF with the smallest eigenvector component in absolute value. The process is repeated until the Ns desired DOFs remain. It is interesting to note that Eq. (33) is nothing more than the transpose of the FIM as given in Eq. (11).

Optimum Sensor Criterion

It is desirable to assess the quality of the selected optimum sensor locations. This is so because it is often likely that multiple sensor placement methods will be implemented, which undoubtedly will yield multiple sensor locations. A criterion then needs to exist to quantify the different locations. Five criteria were investigated by Penny et al.[23] and include the modal assurance criterion, the modified modal assurance criterion, the SVD ratio, the measured energy per mode, and the determinant of the FIM. They suggest the SVD ratio as the best choice. The method computes the ratio of the largest to smallest singular value from an SVD of the eigenvector (modal) matrix reduced to the chosen optimum sensor locations. This modal matrix is obtained from a GR. The best sensor set is the one whose ratio is closest to unity. Once a number of sensor locations are obtained (from the different sensor placement methods), the SVD ratio is evaluated. However, an alternate criterion is now discussed from the model reduction viewpoint.

The exact structural reduction relationship between the master and slave DOFs can be written as

$$\{x_s\} = \left[I - \Omega^2 K_{\text{ss}}^{-1} M_{\text{ss}}\right]^{-1}\left[-K_{\text{ss}}^{-1} K_{\text{sm}} + \Omega^2 K_{\text{ss}}^{-1} M_{\text{sm}}\right]\{x_m\} \tag{34}$$

where subscripts s and m denote the slave and master DOFs, respectively, and Ω is the structural frequency. The binomial series expansion for the first term in Eq. (34) must be of the form[35]

$$\left[I - \Omega^2 K_{\text{ss}}^{-1} M_{\text{ss}}\right]^{-1} = I + A + A^2 + \cdots \tag{35}$$

where $A = \Omega^2 K_{\text{ss}}^{-1} M_{\text{ss}}$. For the expansion in Eq. (35) to be convergent, it is necessary and sufficient that $\|A\| < 1$ or $\|\Omega^2 K_{\text{ss}}^{-1} M_{\text{ss}}\| < 1$ (Refs. 36–38). It can then be shown that the following satisfies this norm requirement:

$$\omega^2_{s,\min} > \Omega^2 \tag{36}$$

where $\omega^2_{s,\min}$ is the minimum eigenvalue from the slave DOF system and Ω^2 is any eigenvalue from the master DOF system. Equation (36) immediately links the master and slave DOF systems and shows that the lowest slave eigenvalue must be greater than any master eigenvalue for the series expansion in Eq. (35) to be valid. If we make the assumption that the master frequency spectrum will be approximately the same irrespective of the sensor placement method, then it is sufficient to maximize $\omega^2_{s,\min}$. Therefore, the best set of locations is the one with the largest $\omega^2_{s,\min}$.

Results

Example 1

The discussed sensor placement methods were implemented for a comparative study on a uniform cantilevered Euler–Bernoulli beam model. The beam was modeled as aluminum with material and geometric properties listed in Table 2. It was discretized into 25 beam 2-DOF/node finite elements (transverse displacement and rotation). The beam had 15 fine mesh elements (with 1/35-m elemental length) from the wall and 10 coarse elements (with 2/35-m elemental length). This reflects a typical finite element mesh where some regions will be finer than others. A consistent mass approach was used to formulate the mass matrix. The first five modes were considered as the target modes, only transverse displacements were considered as the candidate DOF, and a total of 10 desired locations were sought.

The results are shown in Fig. 1. The VI method simply selects the locations with the maximum amplitude from the first five modes. One thing is clearly obvious from Fig. 1: No two methods produce exactly the same set of locations. The poorer methods appear to be PCA, AMKE, and WAMKE, which tended to cluster the sensors toward one side. Those sensor locations will undoubtedly be poor choices because the target mode shapes will look similar from those points. This indicates that the PCA method may be sensitive to the finite element mesh size as is the case for the kinetic energy methods. The other methods tended to separate the sensors, which from an intuitive viewpoint, is more judicious. To quantify each of the locations, the SVD ratio and the proposed $\omega^2_{s,\min}$ value were computed, which are shown in Table 3. For ease of visualization, these values were normalized by their maximum and plotted in Fig. 2. Note that the sensor placement method in the horizontal axis of Fig. 2 refers to the numbers given in parentheses under Method (no.) in Table 3. For the frequency criterion, however, the normalized value was subtracted from one. It is noted that the optimum sensor locations are associated with the smaller normalized values. It is seen that the frequency criterion is somewhat more selective than the SVD ratio in choosing an optimum sensor location. However, both criteria select the reduction approaches as the method of choice, i.e., GR, IRS, and SAR.

Table 2 Material and geometric properties of beam

Property	E, Pa	ρ, kg/m^3	A, m^2	L, m	I, m^4
Value	69×10^9	2710	1.5×10^{-4}	1	4.5×10^{-10}

Table 3 Comparison of sensor placement methods for beam example

Method (no.)	SVD ratio	$\omega^2_{s,\min}$
VI (1)	3.36	1.61×10^7
G-S1 (2)	10.54	3.27×10^6
G-S2 (3)	7.11	1.96×10^6
PCA (4)	28.68	6.59×10^3
GR (5)	2.68	5.40×10^7
IRS (6)	2.29	5.30×10^7
SAR (7)	2.55	6.39×10^7
MPI (8)	5.58	1.69×10^7
ECP (9)	3.49	1.06×10^7
SVD (10)	4.09	1.59×10^7
SF (11)	10.23	2.68×10^5
CI (12)	4.46	6.86×10^6
EFI W/OM (13)	4.09	1.59×10^7
EFI W/M (14)	2.85	1.62×10^7
VEFI (15)	4.28	1.56×10^7
MKE (16)	2.79	1.74×10^7
AMKE (17)	9.34	6.12×10^5
WAMKE (18)	11.35	1.38×10^6
DPR (19)	4.28	2.23×10^7
ADPR (20)	5.52	1.17×10^7
WADPR (21)	8.17	3.56×10^6

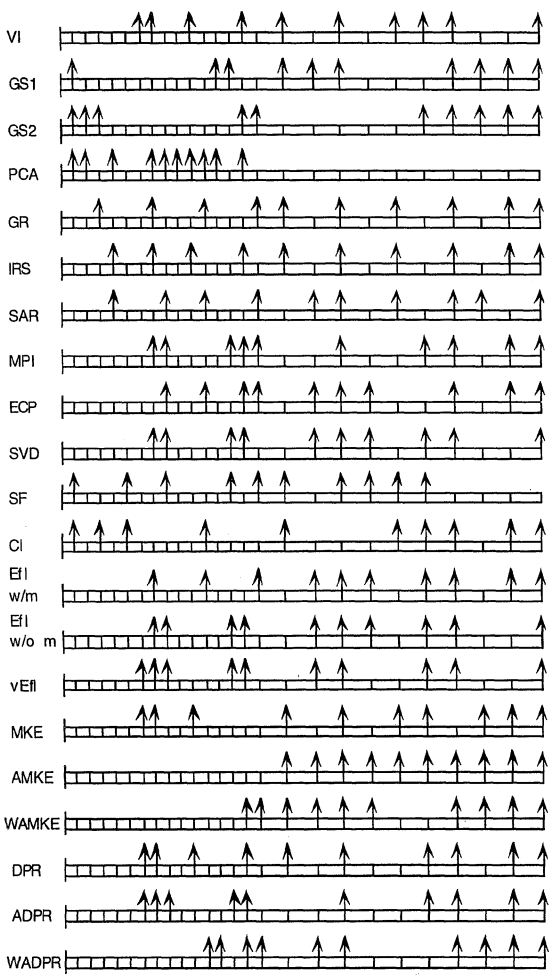

Fig. 1 Optimum beam sensor locations.

Example 2

This example consisted of an experimental cantilevered frame structure, as shown in Fig. 3. The test article, shown schematically in Fig. 4, is 2.5 m in length (from base to tip). The bar elements and nodes are made of aluminum and manufactured by Mero Structures, Inc. The first three FE method bending modes in the Z direction were taken as the target modes and are given in Table 4. Consequently, there were only 15 candidate DOFs, i.e., the Z-displacements at nodes 1–15, from which five sensors were sought.

Table 4 Frame structure target modes in Z direction

Mode	Frequency, Hz	Description
1	23.43	First bending
2	105.10	Second bending
3	208.48	Third bending

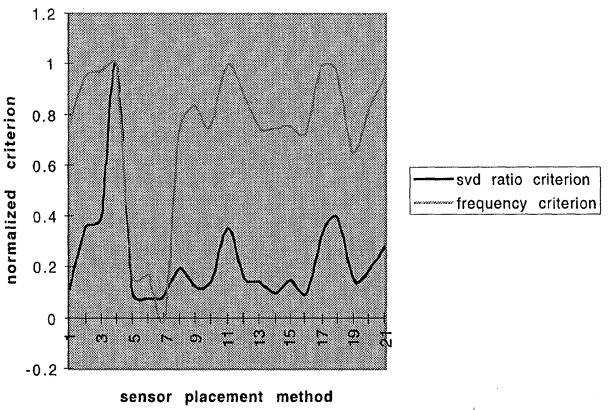

Fig. 2 Plot of sensor criteria vs sensor placement method for beam example.

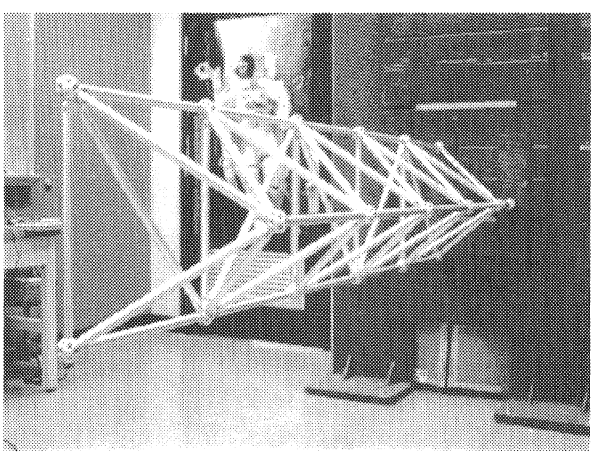

Fig. 3 Cantilevered frame structure.

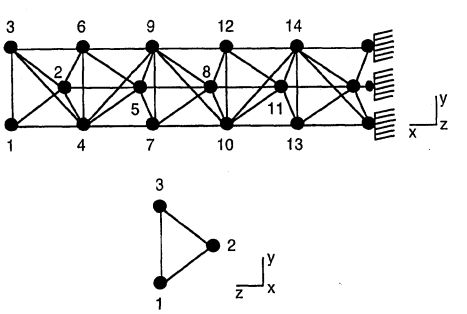

Fig. 4 Frame structure schematic.

An experimental FRF database was available from which the results of the sensor placement methods could be compared. The FRFs were obtained from a single input and were applied at node 11 (Z direction) through a stinger, which was attached to an electromagnetic shaker. The input was random noise, was generated by a Tektronix 2642A Fourier analyzer, and was measured by a force transducer, which was placed between the node and stinger. The input location was fixed throughout all of the tests, whereas the accelerometer was simply moved from point to point. The sampling frequency was 512 Hz and 4096 data points were collected from zero initial conditions.

The frame structure FRFs are shown in Fig. 5. Unfortunately, no analysis could be made with all of the methods because FRFs

Table 5 Experimental frequency-damping errors for frame structure

Method	Mode 1		Mode 2		Mode 3	
	Frequency error, %	Damping error, %	Frequency error, %	Damping error, %	Frequency error, %	Damping error, %
PCA	0.40	26.7	0.37	15.7	0.03	2.8
EFI W/M	0.47	29.9	0.35	20.1	0.01	14.0
ECP	0.49	30.8	0.44	85	0.05	18.8
SF	0.21	23.3	0.48	26.7	0.03	6.8
WAMKE	0.19	24.9	0.47	84.4	0.02	8.1
ADPR	0.61	27.2	0.39	26.0	0.04	5.5
WADPR	0.52	29.9	0.43	77.9	0.04	14.3

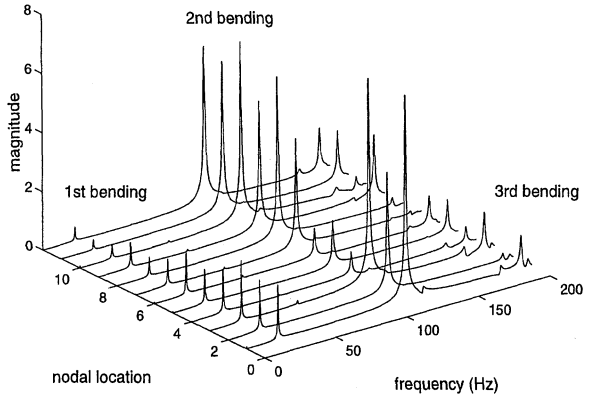

Fig. 5 Frame structure FRFs.

were available only at nodes 1–12. That is, several of the sensor placement methods selected nodes 13 and 14 where no FRF data were available. But seven methods could be investigated, and their frequency-damping errors are shown in Table 5. All 12 FRFs were processed by the ERA to obtain baseline measurements, which were taken to be the exact frequency and damping. A total of 500 data points of the impulse response after a Fourier inversion and a system order of 12 were consistently used for each ERA analysis. As can be seen, the three target frequencies were well recovered, but the damping was somewhat large. However, the third mode produced the lowest errors among the three target modes. The important observation, though, was the overall consistency in the results. That is, no one method was exceedingly superior to any other over all of the three target modes. The large discrepancy in damping for the second mode for ECP, WAMKE, and WADPR is due to noise contamination. Selecting a larger system order provides an avenue for the noise. Increasing the order to 20 in ERA, the damping errors in the second mode become 10.2, 13.8, and 9.02% for ECP, WAMKE, and WADPR, respectively, which are relatively in agreement with the other methods.

Conclusions

Two example structures of varying complexity were investigated for the optimal sensor locations. Numerous sensor placement methods, in addition to the two proposed schemes, were implemented, and the sensor location quality measured using the SVD ratio and a model reduction frequency criterion. The proposed frequency criterion appeared to be more selective than the SVD ratio in selecting the optimum sensors. Furthermore, whereas it was shown that the reduction approach gave good results, most of the methods yielded reasonable results based on a limited experimental study.

References

[1]Juang, J.-N., and Rodriguez, G., "Formulations and Applications of Large Structure Actuator and Sensor Placements," *2nd VPI&SU/AIAA Symposium on Dynamics and Control of Large Flexible Spacecraft Proceedings*, Virginia Polytechnic Inst. and State Univ., Blacksburg, VA, 1979, pp. 247–262.

[2]Baruh, H., and Choe, K., "Sensor Placement in Structural Control," AIAA Paper 88-4056, Aug. 1988.

[3]DeLorenzo, M. L., "Sensor and Actuator Selection for Large Space Structure Control," *Journal of Guidance, Control, and Dynamics*, Vol. 13, No. 2, 1990, pp. 249–257.

[4]Lim, K. B., "Method for Optimal Actuator and Sensor Placement for Large Flexible Structures," *Journal of Guidance, Control, and Dynamics*, Vol. 15, No. 1, 1992, pp. 49–57.

[5]Sanayei, M., Onipede, O., and Babu, S. R., "Selection of Noisy Measurement Locations for Error Reduction in Static Parameter Identification," *AIAA Journal*, Vol. 30, No. 9, 1992, pp. 2299–2309.

[6]Shah, P. C., and Udwadia, F. E., "A Methodology for Optimal Sensor Locations for Identification of Dynamic Systems," *Journal of Applied Mechanics*, Vol. 45, March 1978, pp. 188–196.

[7]Salama, M., Rose, T., and Garba, J., "Optimal Placement of Excitation and Sensors for Verification of Large Dynamical Systems," *AIAA/ASME/ASCE/AHS 28th Structures, Structural Dynamics, and Materials Conference*, AIAA, Washington, DC, 1987, pp. 1024–1031 (AIAA Paper 87-0782).

[8]Schedlinski, C., and Link, M., "An Approach to Optimal Pick-Up and Exciter Placement," *Proceedings of the 14th International Modal Analysis Conference* (Dearborn, MI), Union College Press, Schenectady, NY, 1996, pp. 376–382.

[9]Bayard, D. S., Hadaegh, F. Y., and Meldrum, D. R., "Optimal Experiment Design for Identification of Large Space Structures," *Automatica*, Vol. 24, No. 3, 1988, pp. 357–364.

[10]Basseville, M., Benveniste, A., Moustakides, G. V., and Rougee, A., "Optimal Sensor Location for Detecting Changes in Dynamical Behavior," *IEEE Transactions on Automatic Control*, Vol. AC-32, No. 12, 1987, pp. 1067–1075.

[11]Avitabile, P., Haselton, D., and Moore, J., "Modal Test Reference Selection Using an SVD Procedure," *Proceedings of the 14th International Modal Analysis Conference* (Dearborn, MI), Union College Press, Schenectady, NY, 1996, pp. 1527–1532.

[12]O'Callahan, J., and Li, P., "An Automatic Selection of Reduced Degrees of Freedom," *Proceedings of the 12th International Modal Analysis Conference* (Honolulu, HI), Union College Press, Schenectady, NY, 1994, pp. 481–485.

[13]DeClerck, J. P., and Avitabile, P., "Development of Several New Tools for Modal Pre-Test Evaluation," *Proceedings of the 14th International Modal Analysis Conference* (Dearborn, MI), Union College Press, Schenectady, NY, 1996, pp. 1272–1277.

[14]Kammer, D. C., "Sensor Placement for On-Orbit Modal Identification and Correlation of Large Space Structures," *Journal of Guidance, Control, and Dynamics*, Vol. 14, No. 9, 1991, pp. 251–259.

[15]Larson, C. B., Zimmerman, D. C., and Marek, E. L., "A Comparison of Modal Test Planning Techniques: Excitation and Sensor Placement Using the NASA 8-Bay Truss," *Proceedings of the 12th International Modal Analysis Conference* (Honolulu, HI), Union College Press, Schenectady, NY, 1994, pp. 205–211.

[16]Chung, Y. -T., and Moore, D., "On-Orbit Sensor Placement and System Identification of Space Station with Limited Instrumentations," *Proceedings of the 11th International Modal Analysis Conference* (Kissimmee, FL), Union College Press, Schenectady, NY, 1993, pp. 41–46.

[17]Pape, D. A., "Selection of Measurement Locations for Experimental Modal Analysis," *Proceedings of the 12th International Modal Analysis Conference* (Honolulu, HI), Union College Press, Schenectady, NY, 1994, pp. 34–41.

[18]Tasker, F. A., and Liu, C., "Variance-Based Sensor Placement for Modal Identification of Structures," *Journal of Guidance, Control, and Dynamics*, Vol.18, No. 3, 1995, pp. 627–630.

[19]Garvey, S. D., Friswell, M. I., and Penny, J. E., "Evaluation of a Method for Automatic Selection of Measurement Locations Based on Subspace-Matching," *Proceedings of the 14th International Modal Analysis Conference* (Dearborn, MI), Union College Press, Schenectady, NY, 1996, pp. 1546–1552.

[20]Poston, W. L., "Optimal Sensor Locations for On-Orbit Modal Identification of Large Space Structures," M.S. Thesis, Dept. of Civil, Mechanical, and Environmental Engineering, George Washington Univ., Washington, DC, July 1991.

[21]Park, Y. -S., and Kim, H. -B., "Sensor Placement Guide for Model Comparison and Improvement," *Proceedings of the 14th International Modal Analysis Conference* (Dearborn, MI), Union College Press, Schenectady, NY, 1996, pp. 404–409.

[22]Penny, J. E. T., Friswell, M. I., and Garvey, S. D., "The Automatic Choice of Measurement Locations for Dynamic Testing," *Proceedings of the 10th International Modal Analysis Conference* (San Diego, CA), Union College Press, Schenectady, NY, 1992, pp. 30–36.

[23]Penny, J. E. T., Friswell, M. I., and Garvey, S. D., "Automatic Choice of Measurement Locations for Dynamic Testing," *AIAA Journal*, Vol. 32, No. 1, 1994, pp. 407–414.

[24]Henshell, R. D., and Ong, J. H., "Automatic Masters for Eigenvalue Economization," *Earthquake Engineering and Structural Dynamics*, Vol. 3, No. 4, 1975, pp. 375–383.

[25]Shah, V. N., and Raymund, M., "Analytical Selection of Masters for the Reduced Eigenvalue Problem," *International Journal of Numerical Methods in Engineering*, Vol. 18, No. 1, 1982, pp. 89–98.

[26]Guyan, R. J., "Reduction of Stiffness and Mass Matrices," *AIAA Journal*, Vol. 3, No. 2, 1965, p. 380.

[27]O'Callahan, J., "A Procedure for an Improved Reduced System (IRS) Model," *Proceedings of the 7th International Modal Analysis Conference* (Las Vegas, NY), Union College Press, Schenectady, NY, 1989, pp. 17–21.

[28]Zhang, D.-W., and Li, S., "Succession-Level Approximate Reduction (SAR) Technique for Structural Dynamic Model," *Proceedings of the 13th International Modal Analysis Conference* (Nashville, TN), Union College Press, Schenectady, NY, 1995, pp. 435–441.

[29]Flanigan, C. C., and Botos, C. D., "Automated Selection of Accelerometer Locations for Modal Survey Tests," *Proceedings of the 10th International Modal Analysis Conference* (San Diego, CA), Union College Press, Schenectady, NY, 1992, pp. 1205–1208.

[30]Johnson, C. L., and Mack, N., "Accelerometer Selection for the Modal Survey of the Space Station Combined Cargo Element," *Proceedings of the 12th International Modal Analysis Conference* (Honolulu, HI), Union College Press, Schenectady, NY, 1994, pp. 1230–1236.

[31]Lim, T. W., "Actuator/Sensor Placement for Modal Parameter Identification of Flexible Structures," *International Journal of Analytical and Experimental Modal Analysis*, Vol. 8, No. 1, 1993, pp. 1–13.

[32]Juang, J.-N., and Pappa, R. S., "An Eigensystem Realization Algorithm for Modal Parameter Identification and Model Reduction," *Journal of Guidance, Control, and Dynamics*, Vol. 8, No. 5, 1985, pp. 620–627.

[33]Haykin, S., *Neural Networks: A Comprehensive Foundation*, Macmillan College Pub., Englewood Cliffs, NJ, 1994, pp. 363–369.

[34]Meirovitch, L., *Computational Methods in Structural Dynamics*, Sijthoff and Noordhoff, Rockville, MD, 1980, pp. 8–10.

[35]Gordis, J. H., "An Analysis of the Improved Reduced System (IRS) Model Reduction Procedure," *International Journal of Analytical and Experimental Modal Analysis*, Vol. 9, No. 4, 1994, pp. 269–285.

[36]Flax, A. H., "Comment of 'Reduction of Structural Frequency Equations,'" *AIAA Journal*, Vol. 13, No. 5, 1975, pp. 701, 702.

[37]Kidder, R. L., "Reply by Author to A. H. Flax," *AIAA Journal*, Vol. 13, No. 5, 1975, pp. 702, 703.

[38]Flax, A. H., "Comment of 'Dynamic Condensation,' " *AIAA Journal*, Vol. 23, No. 11, 1985, pp. 1841–1843.

A. D. Belegundu
Associate Editor